ANNUAL REVIEWS

Annual Review of Neuroscience

Integration of Feedforward and Feedback Information Streams in the Modular Architecture of Mouse Visual Cortex

Andreas Burkhalter,[1] Rinaldo D. D'Souza,[1] Weiqing Ji,[1] and Andrew M. Meier[2]

[1]Department of Neuroscience, Washington University School of Medicine, St. Louis, Missouri, USA; email: burkhala@wustl.edu

[2]Department of Speech, Language, and Hearing Sciences, College of Engineering, Boston University, Boston, Massachusetts, USA

Annu. Rev. Neurosci. 2023. 46:259–80

First published as a Review in Advance on March 27, 2023

The *Annual Review of Neuroscience* is online at neuro.annualreviews.org

https://doi.org/10.1146/annurev-neuro-083122-021241

Keywords

patchy connections, layer 1, processing streams, M2 muscarinic acetylcholine receptor, processing hierarchy

Abstract

Radial cell columns are a hallmark feature of cortical architecture in many mammalian species. It has long been held, based on the lack of orientation columns, that such functional units are absent in rodent primary visual cortex (V1). These observations led to the view that rodent visual cortex has a fundamentally different network architecture than that of carnivores and primates. While columns may be lacking in rodent V1, we describe in this review that modular clusters of inputs to layer 1 and projection neurons in the layers below are prominent features of the mouse visual cortex. We propose that modules organize thalamocortical inputs, intracortical processing streams, and transthalamic communications that underlie distinct sensory and sensorimotor functions.

Contents

INTRODUCTION 260
NONRANDOM ARCHITECTURE OF MOUSE VISUAL CORTEX 261
SUBCORTICAL CONNECTIONS WITH V1 MODULES 266
Geniculocortical Network 266
Colliculo-Thalamo-Cortical Network 268
CORTICAL CONNECTIONS WITH V1 MODULES 269
Modular Dorsal and Ventral Cortico-Cortical Networks 269
Functional Architecture of Dorsal and Ventral Intracortical Networks 269
TRANSTHALAMIC NETWORK 271
CORTICAL HIERARCHY 272

INTRODUCTION

Radial cell columns are a hallmark feature of cortical architecture in many mammalian species (Molnár & Rockland 2020). The modular design of periodically arranged columns and cell clusters in the tangential plane minimizes axon length and saves space (Chklovskii & Koulakov 2004). While this modular design optimizes networks, columns and modules are unexpectedly absent in primary visual cortex (V1) of some primate species (Adams & Horton 2009). Thus, the function of columns remains controversial (Horton & Adams 2005). There is, however, agreement that columnar and modular cell clusters group similar response properties and subdivide the network for routing information into different processing streams (Horton & Adams 2005). It has long been held, based on the lack of orientation columns (Girman et al. 1999, Ohki & Reid 2007, Ohki et al. 2005, Scholl et al. 2013, Van Hooser et al. 2005), that such functional units are absent in rodent V1. This belief led to the view that rodent visual cortex, and presumably all of neocortex, has a different architecture than that of carnivores and primates. This difference raises the question of whether mice are suitable models for deciphering the synaptic basis of human cortical brain disorders (Loomba et al. 2022).

While columns may be lacking in mouse V1, modularity may exist in the organization of the extended cortical network. Clustering of neurons is a key feature of the primate visual system (Vanni et al. 2020) and a fundamental property of population coding, by which stimuli of the outside world are represented by the correlated activity of nearby neurons (Berry & Tkacik 2020). Recently, clustered correlated activity was found to play a role in the assembly of the visual system in mice (Murakami et al. 2022). Wide-field calcium imaging in 5–14-day-old pups showed that spontaneous retinal activity drives inputs to the dorsal lateral geniculate nucleus (dLGN) and the posterior and anterior lateral posterior nucleus (pLP and aLP) and sculpts the hierarchical network, including the diverse processing streams of visual cortex (D'Souza et al. 2022, Murakami et al. 2022, Wang et al. 2012). Although the modularity of these bottom-up pathways is critical for development and the construction of basic visual representations in lower and higher cortical areas (Roelfsema 2006), feedforward (FF) connections are insufficient for visual perception. For example, figure-ground segregation, filling in surfaces, selecting parts of the image for spatial attention, integrating sensory modalities, computing distance from optic flow and running speed during spatial navigation, and detecting visuomotor mismatch to distinguish external visual motion from that produced by the body's own motion all depend on top-down processing (Chaplin & Margrie 2020, Khan & Hofer 2018, Keller & Mrsic-Flogel 2018, Roelfsema & de Lange 2016, Saleem 2020,

Saleem et al. 2013). The diverse signals are generated by communications between the cortex and thalamus, interactions within recurrent cortical networks that involve inputs from horizontal intra-areal connections, and interareal feedback (FB) pathways from hierarchically higher areas, which in monkeys and mice are modular (Bennett et al. 2019, D'Souza et al. 2019, Federer et al. 2021, Ji et al. 2015, Siu et al. 2021). The physiological effects of these interactions can be modulatory (attention), enhancing (mental imagery), or strong enough to cancel external sensory inputs (hollow face illusion) (Vezoli et al. 2021). This diversity of top-down effects may be due to the modular organization of the network and/or module-specific synaptic mechanisms. Understanding such networks in mice seems relevant to human perception and cognition.

Recent findings of clustered M2 muscarinic acetylcholine receptor (M2) expression in layer 1 (L1) suggest that some form of modularity is expressed in the synaptic organization of mouse V1 (Ji et al. 2015) (**Figures 1*a–c*** and **2*b***). The modular motif of M2-positive patches (P_{M2+}) and M2-negative interpatches (IP_{M2-}) extends to spatially segregated inputs from the dLGN and interdigitating projections from the LP to L1 of V1 (D'Souza et al. 2019, Ji et al. 2015) (**Figure 2*c*,*d***). Importantly, the modularity includes clustered reciprocal long-range connections between V1 and higher cortical areas (D'Souza et al. 2019, 2022; Ji et al. 2015; Meier et al. 2021).

Here we review anatomical and physiological evidence for a modular architecture of the mouse visual system. We propose, based on M2 clustering and the patchy connectivity of V1 L1, that bottom-up thalamocortical inputs and intracortical FB are selective for P_{M2+} or IP_{M2-}. The modular organization is widespread but not present throughout visual cortex (Meier et al. 2021). It includes auditory cortex and extends to parahippocampal areas whose cognitive functions are controlled by the amygdala (Burgess et al. 2016, Ramesh et al. 2018). The modularity further subdivides the ventral (what) processing stream specialized for object recognition and the dorsal (where) stream for processing visual motion information (Wang et al. 2011, 2012) into a ventral P_{M2+} and two dorsal subnetworks designated as the posterior-parietal P_{M2+} and medial IP_{M2-} substreams. The dorsal P_{M2+} substream receives optic flow information generated in the retina (Marques et al. 2018, Sit & Goard 2020), encoded in an eye-centered reference frame, while the IP_{M2-} substream computes the direction of optic flow more centrally in a body-centered frame (Meyer et al. 2020). The dorsal P_{M2+} substream linked through cortico-thalamo-cortical (transthalamic) (Sherman & Guillery 2011) connections plays a role in the discrimination of external cues from self-generated visual FB, while the transthalamic connections of the dorsal IP_{M2-} substream process high-spatial-frequency visuomotor signals (Blot et al. 2021). Thus, the mouse visual cortical hierarchy is a network comprising distinct processing streams and modules of cells with dissimilar synaptic connections.

NONRANDOM ARCHITECTURE OF MOUSE VISUAL CORTEX

The proposed modular architecture of M2 expression in L1 of mouse V1 (Ji et al. 2015) is not entirely unexpected. A comparable modularity was observed almost 20 years ago in rat V1 (Ichinohe et al. 2003). In looking at vesicular glutamate transporter 2 (VGluT2)- and parvalbumin (PV)-immunostained tangential sections through L1/2, Ichinohe et al. (2003) found that the patterns of putative thalamocortical input and subtypes of inhibitory neurons were clustered, periodic, and distributed in interdigitating patches with a center-to-center spacing of 50–120 μm (**Figure 2*a***). Similar images were obtained later from L1 of mouse V1, where the PV+ neuropil alternated with a mutually exclusive pattern of M2 expression (D'Souza et al. 2019). Pathway tracing experiments showed that $IP_{M2-/PV+}$ received input from the LP, whereas $P_{M2+/PV-}$ were targeted by axons from the dLGN (D'Souza et al. 2019, Ji et al. 2015) (**Figure 2*c*,*d***). Although the focus here is on L1, we should point out that the dLGN also projects to L2/3, 4, and 5B and LP to L5A (Zhou et al. 2018). Notably, the M2 pattern is observed as early as postnatal day 4, one week before eye

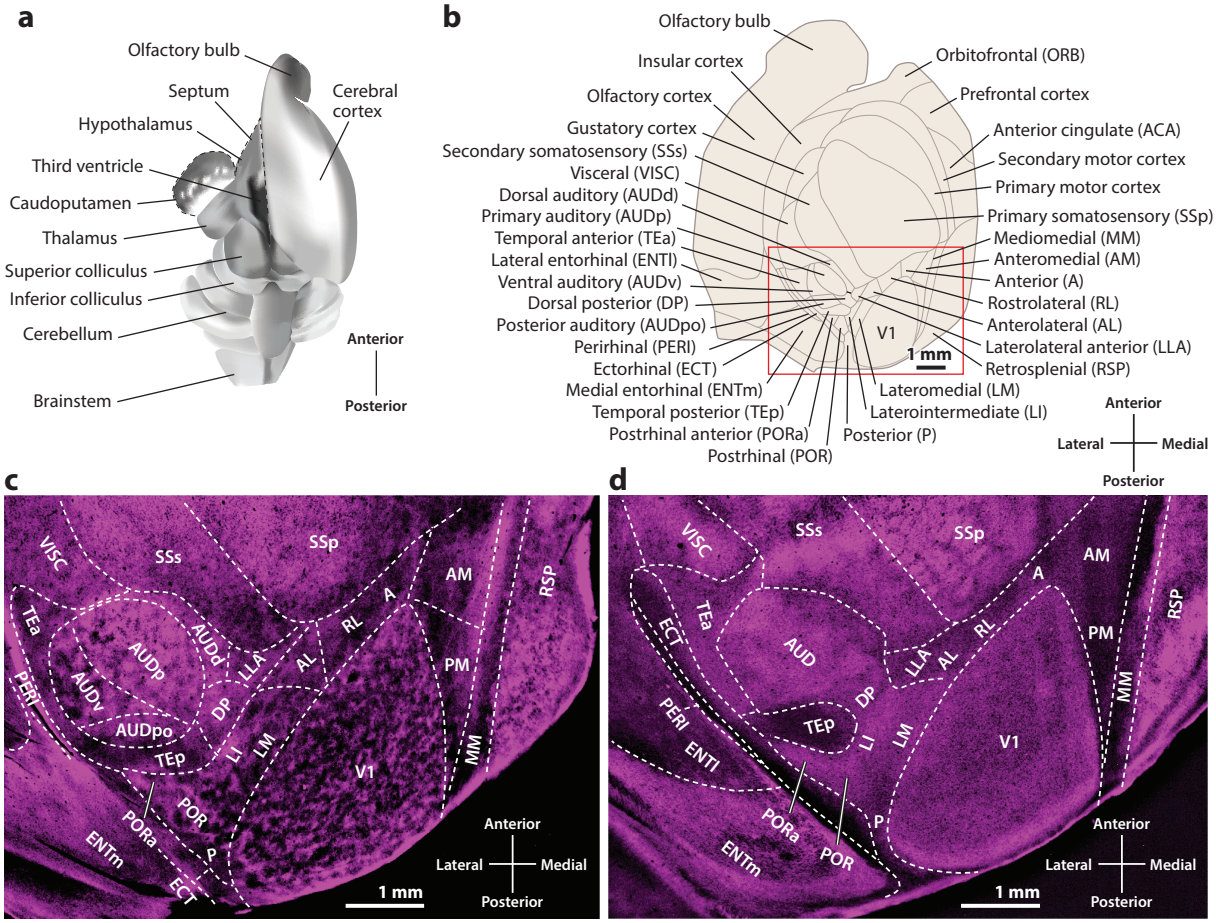

Figure 1

Modular tangential architecture of mouse visual cortex. (*a*) To reveal the patchy organization in layer 1 of mouse visual cortex, the brain is first lightly fixed. Next, the cerebral cortex is separated from the caudoputamen, nucleus accumbens, hypothalamus, and the thalamus. The cortex is then physically unfolded to reveal all buried parts and display the tissue as a single sheet. Finally, the flat-mounted tissue is postfixed and cut on a freezing microtome at 40 μm in the tangential plane. (*b*) The diagram of a tangential section through left cerebral cortex shows areas identified by immunostaining with antibodies against the M2 muscarinic acetylcholine receptor. Panel *b* adapted from Gămănuţ et al. (2018). (*c*) The fluorescent image of a tangential section through layer 1 stained with an antibody against M2 muscarinic acetylcholine receptor shows patchy M2 expression in primary visual cortex (V1), select areas of surrounding higher visual cortex, and auditory and retrosplenial cortex. The image was taken at a location outlined by the red box in panel *b*. (*d*) The image shows uniform M2 staining of visual cortex in layer 4. Panels *c* and *d* adapted from Meier et al. (2021).

opening (D'Souza et al. 2019) (**Figure 3*a–c***). The pattern is not unique to mice and is present in rat and macaque monkey V1, where the P_{M2+} modules in L1 were aligned with cytochrome oxidase (CO)-poor interblobs of L2/3 (Ji et al. 2015) (**Figure 3*d–f***). Whether this arrangement is of any functional significance is unclear and awaits the determination of the spatial relationships between M2, CO, and thalamocortical inputs to rodent V1.

L1 is cell sparse but contains axons and dendritic tufts of pyramidal cells (PCs), whose cell bodies lie in L2–6. To identify the cellular elements that express M2, Mrzljak et al. (1996) and Disney et al. (2006) analyzed immunostained tissues from L2/3, L4A, and L4Cβ of macaque V1 under the electron microscope. They found that M2 is associated with presynaptic geniculocortical and

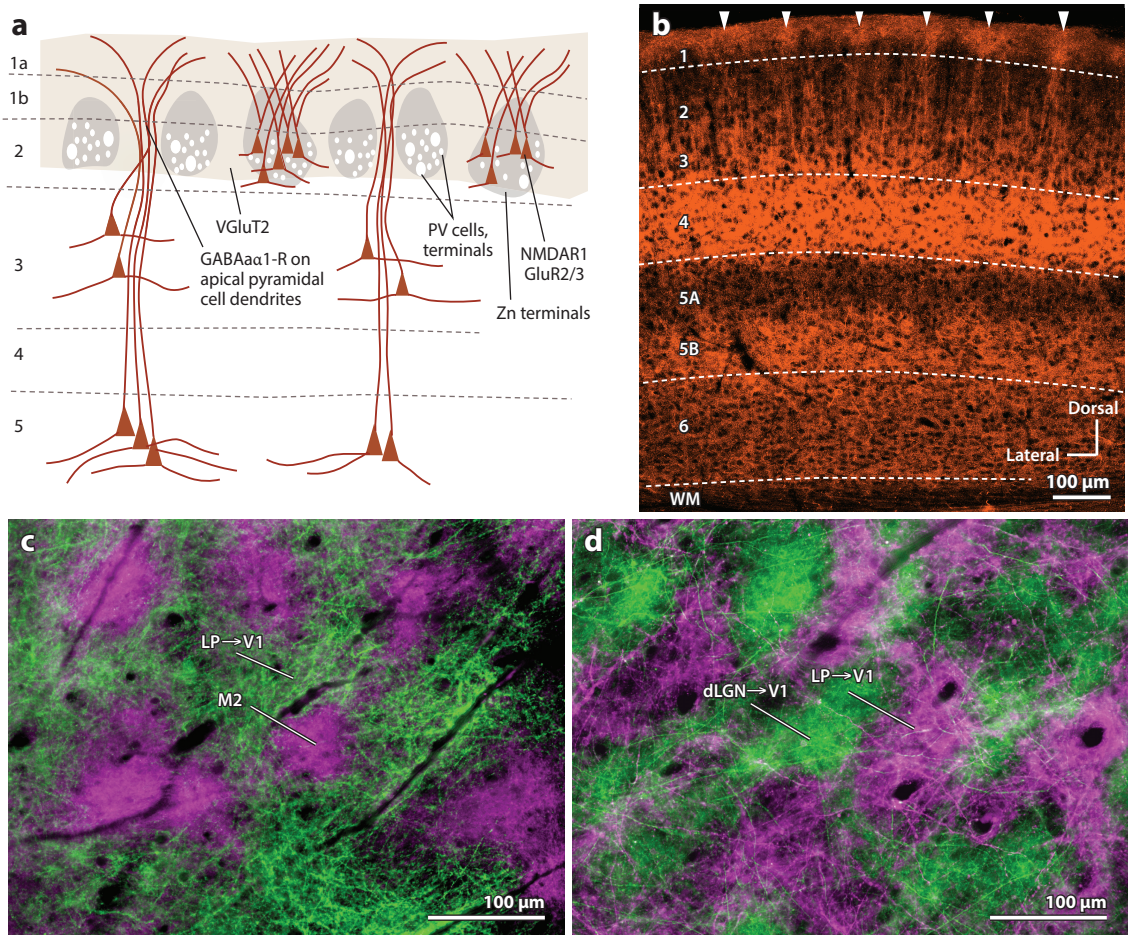

Figure 2

Modular vertical architecture and patchy thalamocortical input to layer 1 of mouse primary visual cortex (V1). (*a*) Graphical depiction of coronal section through layers 1–5 of rat V1. The scheme shows ∼80-µm-wide patches of parvalbumin (PV)-expressing cells and axon terminals (*large* and *small white dots*) alternating periodically with PV-negative clusters (*tan*). The PV-positive patches are colocalized with glutamate receptor 2/3 (GluR2/3)- and *N*-methyl-D-aspartate receptor 1 (NMDAR1)-expressing pyramidal cell bodies (*red*) surrounded by zinc-labeled axon terminals of putative intracortical connections (*gray*). The PV-negative patches contain apical dendrites of pyramidal cells, which express GABAaα1 receptors (GABAaα1-Rs) (*tan*) and are surrounded by vesicular glutamate transporter 2 (VGluT2) immunoreactive putative geniculocortical axon terminals (*tan*). Panel *a* adapted with permission from Ichinohe et al. (2003). (*b*) Laminar distribution of M2 muscarinic acetylcholine receptor (M2) expression in coronal section of mouse V1. In layer 1, M2 shows a nonuniform patchy tangential pattern (*white arrow heads*) reminiscent of apical dendritic tufts ascending from pyramidal cells in deeper layers. M2 expression in layers 4 and 5B is uniform. The white matter (WM) shows no detectable M2 staining. Panel *b* adapted from Ji et al. (2015). (*c*) Tangential section through layer 1 of mouse V1 showing M2 expression in M2-positive patches (*magenta*) interdigitating with axonal projections from the thalamic lateral posterior nucleus (LP) labeled by anterograde tracing with AAVs (*green*). (*d*) Tangential section through layer 1 of mouse V1 showing interdigitating patchy patterns of inputs from the dorsal lateral geniculate nucleus (dLGN) (*green*) and the LP (*magenta*) labeled by anterograde tracing with AAVs. Panels *c* and *d* adapted from D'Souza et al. (2019).

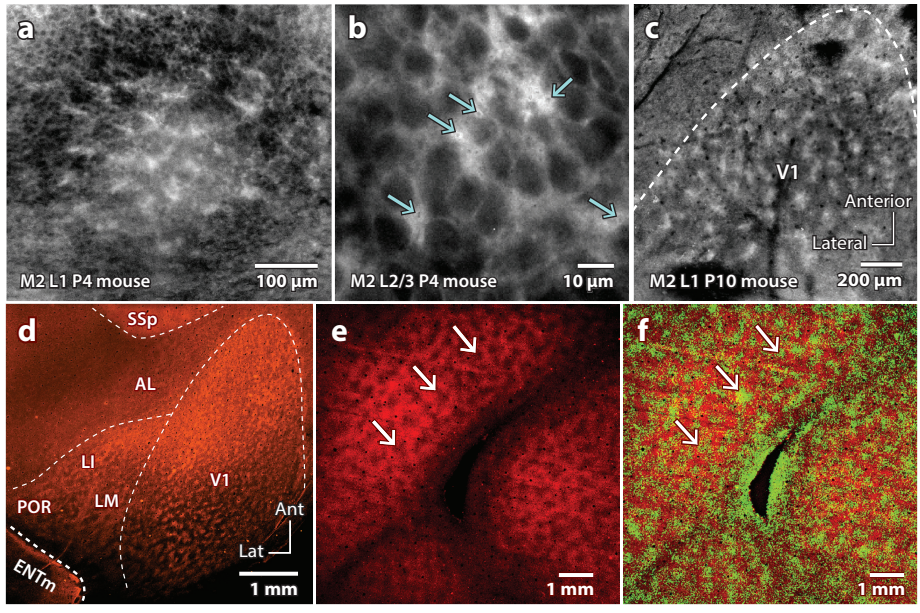

Figure 3

Development and expression of M2 muscarinic acetylcholine receptor (M2) in rat and monkey primary visual cortex (V1). (*a*) Tangential sections through V1 show patchy expression of M2 in layer 1 (L1) of 4-day-old Chrm2tdT mouse. (*b*) At higher magnification, membrane-bound M2 expression in L2/3 shows rings of cross-sectioned dendritic bundles (*arrows*) occupying spaces between unlabeled cell bodies. (*c*) A patchy pattern of M2 immunolabeling in L1 of a 10-day-old C57BL/6 mouse is shown. (*d*) Tangential section through L1 of adult rat visual cortex stained with an antibody against M2 shows patchy expression in V1, lateromedial (LM), anterolateral (AL), laterointermediate (LI), and postrhinal (POR) cortex. M2 expression is also shown in medial entorhinal cortex (ENTm) and primary somatosensory barrel cortex (SSp). Scale bar: 1 mm. (*e*) Tangential section through L1 of macaque monkey V1 stained with an antibody against M2 shows patchy immunolabeling. Arrows indicate matching locations in panels *e* and *f*. (*f*) Complementary patterns of M2+ patches (*red*) in L1 and cytochrome oxidase blobs in L2/3 (*green*). Scale bar: 1 mm. Panels *a–c* adapted from D'Souza et al. (2019), and panels *d–f* adapted from Ji et al. (2015).

GABAergic terminals, boutons of cholinergic axons, dendritic spines of PCs, and thin dendrites of interneurons. From these studies we assume that M2 in L1 of mouse V1 labels similar elements of the neuropil. Thus, it appears that P_{M2+} and IP_{M2-} are innervated by axons from different pathways, which contact the apical dendrites of distinct types of PCs and inhibitory neurons (Karimi et al. 2020).

Orderly maps in which different neuronal response properties are grouped into modules that are arranged periodically in the tangential plane are well-known features of the visual cortex of many nonrodent mammalian species (Molnár & Rockland 2020). Such maps include the representation of the eyes in separate domains of L4, pinwheel representations of orientation preferences in L2/3, and luminance polarity (responsivity to light and dark stimuli) in patches of L4 (Kremkow et al. 2016, Ohki et al. 2006, Scholl et al. 2013). Central players in setting up such maps are retinotopic projections from the thalamus (Kremkow et al. 2016, Nauhaus & Nielsen 2014). Why orderly maps are less common in rodents has been a puzzle. In the absence of answers, many researchers accepted that the architecture of the rodent visual cortex is random; however, recent findings began to challenge this idea. One example comes from observations in rat that intraocular injections of an anterograde transneuronal tracer label approximately 250-µm-wide eye-specific

domains in L4 of the binocular zone of ipsilateral V1 (Laing et al. 2015). The clusters are reciprocally connected through the corpus callosum and may integrate interhemispheric and ipsilateral inputs from the binocular visual field.

In carnivores and primates, the functional architecture of V1 is governed by the convergence of thalamocortical inputs with distinct response properties at specific locations of the cortical sheet. The diverse afferent signals are precisely matched in retinotopy, eye preference, and sensitivity to the onset (ON) and offset (OFF) of light. Studies in several mammalian species have shown that RFs of simple cells are generated by the alignment of ON and OFF geniculocortical inputs. Inputs to V1 of different strengths and topographic alignment are combined in partially overlapping subregions of opposite polarity (Smith & Häusser 2010), which make RFs sensitive to oriented edges (Bonin et al. 2011, Jin et al. 2011, Lien & Scanziani 2013). The topology of ON and OFF inputs predicts the columnar architecture of orientation-selective neurons in monkey, cat, ferret, and tree shrew V1 (Lee et al. 2016, Paik & Ringach 2011). Thus, in mice, which lack orientation maps (Ohki & Reid 2007), one expects (for alternative expectation, see Pattadkal et al. 2018) ON and OFF responses to be distributed in a salt-and-pepper organization, but the evidence tells a different story. Mapping calcium responses of L2/3–4 PC somata in awake TRE-GCaMP6s × CaMKII-tTA mice, Tring et al. (2022) found that ON and OFF responses in V1 were distributed in distinct 60-μm-wide clusters. ON and OFF domains showed an interdigitating tangential pattern, which mirrored shifts in the densities of ON/OFF inputs in the visual field. Notably, the size, spacing, and overall distribution of ON/OFF domains showed a striking similarity to the M2+/M2− pattern in L1 (Ji et al. 2015), suggesting that apical dendrites of ON and OFF cells in L2–4 target distinct compartments of L1. Why then are the orderly ON/OFF maps not translated into orderly orientation maps? A possible answer comes from a model of Nyquist sampling of topographic information contained in the retinal mosaic and the cortex (Jang et al. 2020). The comparison showed that if the sampling ratio between the number of retinal ganglion cells (GCs) and cortical neurons is small, as in rabbits, squirrels, rats, and mice, orientation preferences are intermingled like salt and pepper. In contrast, larger ratios, as in the ferret, tree shrew, cat, and macaque, result in orderly orientation maps.

The notion of the noncolumnar architecture of mouse V1 originated from unit recordings on tracks perpendicular to the pial surface, which showed that neurons with similar orientation preferences were rare (Dräger 1975, Mangini & Pearlman 1980). However, columns could easily be missed if recordings veered off track. To address this, calcium recordings showed that L2/3 and L5 cells with similar orientation preferences were often aligned in 10–40-μm-wide cylinders (Kondo et al. 2016, Maruoka et al. 2017, Ringach et al. 2016). Apical dendrites of similarly tuned cells aggregated to <10-μm-wide bundles, which were joined by neighboring bundles with different orientation preferences, before they branched into 100–200-μm-wide tufts in L1 (Kondo et al. 2016). Bundling of dendrites and exchange between bundles matched descriptions of microtubule associated protein 2 (MAP2) immunostained microcolumns in mouse barrel cortex and rat V1 (Escobar et al. 1986, Peters & Kara 1987). Thus, dendritic clusters in L1 presumably represent multiple orientations, suggesting that they are not vestiges of orientation columns.

In the tangential plane, orientation-selective neurons in L5 are organized in multiple overlapping, spatially offset hexagonal lattices with a grid size of approximately 30 μm (Maruoka et al. 2017). Each grid represents different projection neurons with distinct connections. For instance, one such population has recently been identified as *Tlx3* (T cell leukemia homeobox 3)-expressing intracortically projecting and another as subcortically projecting to the superior colliculus (SC) and the pons (Maruoka et al. 2017). It is possible that the spatially clustered domains in L2/3–4, which are biased for ON and OFF responses (Tring et al. 2022), are aligned with the grid in L5 (Maruoka et al. 2017). If so, OFF responses, which are often stronger, faster, and more salient

than ON responses (Williams et al. 2021), may be distributed preferentially across the M2 scaffold and confer differential sensitivities to intracortical and subcortically projecting neurons (Maruoka et al. 2017). Each grid may contain neurons that project spatially expanding (from 30 μm in L5 to 80 μm in L1) bouquets of apical dendrites preferentially to P_{M2+} and IP_{M2-} in L1 (Meier et al. 2021). V1 inputs from the dLGN shell, the superficial part of the nucleus that targets L1 (Cruz-Martín et al. 2014), may influence cells projecting to the higher visual areas LM (lateromedial) and AL (anterolateral) through dendrites in P_{M2+}, whereas inputs from the LP may contact cells that project to the higher-area PM (posteromedial) with dendrites in IP_{M2-} (D'Souza et al. 2019, Ji et al. 2015) (**Figure 1*b***). Thus, P_{M2+} and IP_{M2-} may group cells with distinct ON/OFF biases into distinct output units (Innocenti & Vercelli 2010).

SUBCORTICAL CONNECTIONS WITH V1 MODULES

The knowledge that image-forming visual information reaches the cortex through two visual systems goes back to studies in hamster, which showed that discriminative vision is linked to the geniculocortical (retina→dLGN→V1) pathway whereas visually guided orienting of body, head, and eyes is associated with the colliculo-thalamo-cortical channel (Schneider 1969) (**Figure 4**). The more indirect colliculo-thalamo-cortical pathway ascends via the SC and the higher-order LP, which is richly interconnected with the striatum and the amygdala (Tohmi et al. 2014, Zhou et al. 2018). Although introduced here as parallel pathways, it is important to note that they are linked through SC→dLGN connections, which have a functional impact on the spatial integration of V1 neurons (Ahmadlou et al. 2018, Bickford et al. 2015).

Geniculocortical Network

The notion that visual features are extracted in modular circuits with columnar architecture originated with the identification of interdigitating eye-specific geniculocortical projections to L4 of cat and primate V1 (da Costa & Martin 2010). No such eye-dominance bands have been observed in mice, where monocular transneuronal pathway tracing produced uniform labeling in L4 of V1, even though inputs from the ipsi- and contralateral retina are segregated in distinct domains of the dLGN core (Dräger 1974, Morin & Studholme 2014). Evidently, modular maps in mouse V1 (D'Souza et al. 2019, Ji et al. 2015) are unlikely to be a simple recapitulation of the laminar organization of retinal inputs to the dLGN, its projections to L4, and downstream connections to L2/3 (Nauhaus & Nielsen 2014). While L4 is the main target of dLGN input to V1, geniculocortical projections also terminate in L1, 2/3, 5, and 6 (Roth et al. 2016, Zhou et al. 2018). Inputs to L2/3–6 originate in the dLGN core and are uniformly distributed in the tangential plane. In contrast, inputs to L1 arise from the dLGN shell (Cruz-Martín et al. 2014) and terminate in distinct patches (Ji et al. 2015) (**Figure 2*d***). Projections to L1 are not unique to mouse V1; they also exist in primates, where they originate from koniocellular layers of the magnocellular dLGN and terminate in a nonuniform pattern in L1 (Casagrande et al. 2007, Fitzpatrick et al. 1983). Unlike dLGN core inputs to L4, which in mouse V1 synapse onto basal dendrites of PCs (Scala et al. 2019), inputs to L1 contact apical dendrites of PCs (Karimi et al. 2020) and interneurons (Cohen-Kashi Malina et al. 2021, Jiang et al. 2013, Pardi et al. 2020). Inputs at this location play little role in the generation of stimulus-selective responses (Park et al. 2019). Rather, L1 inputs gate the pattern and firing frequency and decrease response variability of select groups of intratelencephalic- and pyramidal tract–projecting neurons in mouse primary visual and somatosensory cortex (Cohen-Kashi Malina et al. 2021, Doron et al. 2020, Egger et al. 2015).

The central projections of the mouse retina originate in more than 40 different types of GCs (Goetz et al. 2022), which terminate in 59 targets with the strongest inputs to the dLGN and

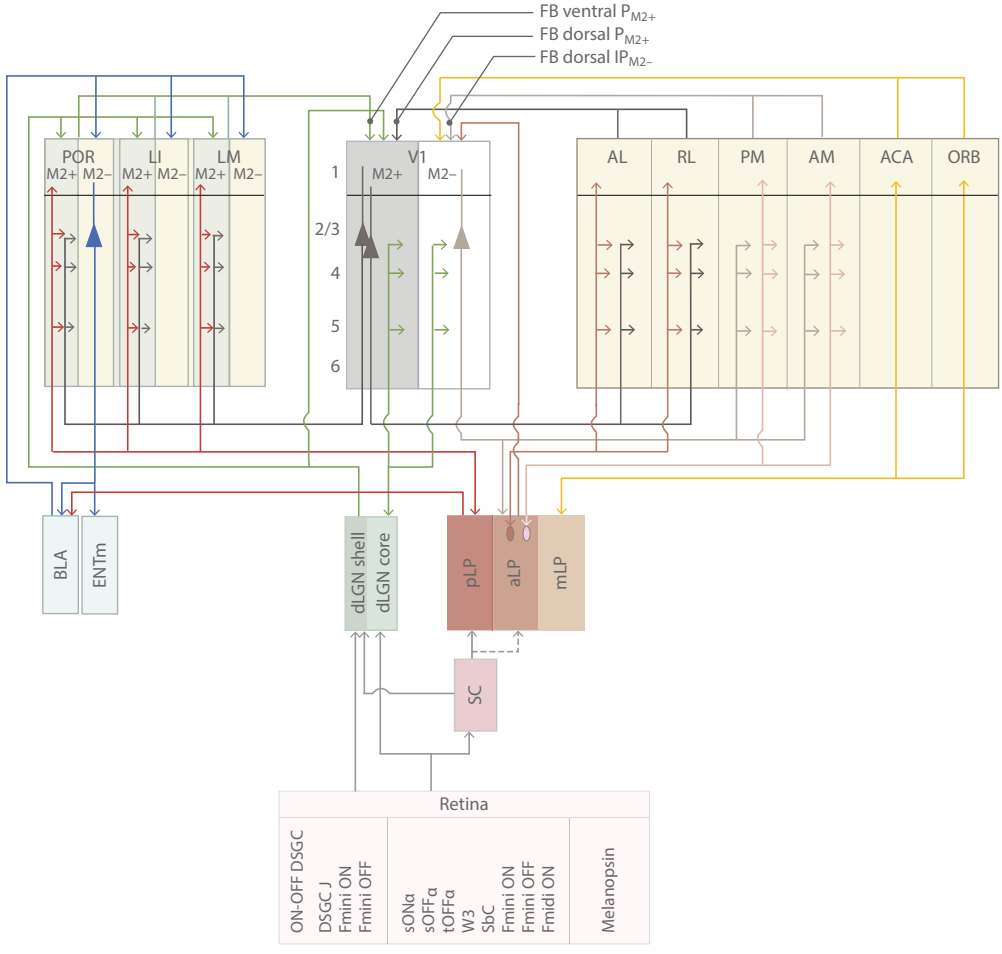

Figure 4

Circuit diagram of the integration of feedforward and feedback information streams in the modular architecture of the mouse visual system. The diagram is derived from the clustered inputs of P_{M2+} and IP_{M2-} to L1 of V1, LM, LI, P, and, POR. It draws from evidence that apical dendrites of pyramidal cells in the layers below often overlap with patchy inputs to L1, indicating looped like-to-like reciprocal circuits. While suggestive, it is important to note that synaptic connectivity has not been established, except for a few specific cases discussed in the text. The diagram highlights the mesoscopic organization and oversimplifies connection preferences as unambiguous target-specific connections. Importantly, the diagram provides no explicit information about the synaptic network organization between pyramidal cells, contacts between pyramidal cells, and different types of inhibitory neurons or connections between interneurons. Note that the list of retinal ganglion cells is incomplete and limited to the most common subtypes. The diagram shows module-selective thalamic and cortical input to L1, like-to-like intracortical loops, segregation of cortical streams, segregation of retina- and more centrally generated optic flow signals, transthalamic loops to distinguish optic flow from self-generated movements and other visuomotor signals, and interactions with the amygdala and the ENTm. The connecting lines with arrows at both ends indicate validated reciprocal connections. Lines with a single arrow indicate that reciprocity is unknown. Abbreviations: ACA, anterior cingulate area; AL, anterolateral; aLP, anterior LP; AM, anteromedial; BLA, basolateral amygdala; dLGN, dorsal lateral geniculate nucleus; DSGC J, direction-selective ganglion cell enriched in junctional adhesion molecule JAM-B; ENTm, medial entorhinal cortex; FB, feedback; Fmini ON/Fmini OFF, direction-selective retinal ganglion cells expressing transcription factor Foxp2; IP_{M2-}, M2-negative interpatch; L, layer; LI, laterointermediate; LM, lateromedial; LP, lateral posterior nucleus; M2, M2 muscarinic acetylcholine receptor; mLP, medial LP; ON-OFF DSGC, ON-OFF direction–selective ganglion cell; ORB, orbitofrontal; P, posterior area; pLP, posterior LP; PM, posteromedial; P_{M2+}, M2-positive patch; POR, postrhinal; RL, rostrolateral; SbC, suppressed by contrast; SC, superior colliculus; sONα, sOFFα, tOFFα, sustained (s), transient (t) large, non-direction-selective ganglion cells; V1, primary visual cortex; W3, retinal ganglion cells sensitive to small moving objects on featureless background.

SC (Martersteck et al. 2017). More than 80% of dLGN-projecting GCs send axon collaterals to the SC (Ellis et al. 2016). Most types of GCs project to the dLGN, where inputs are sorted and combined in the core and shell in cell type–specific fashion. Considering the vast functional diversity of GCs, dLGN responses reflect inputs from an unexpectedly small number of GC types, likely two to five, each responding to the presence and absence of light and showing regular tiling across the retina (Baden et al. 2016, Goetz et al. 2022, Kerschensteiner 2022, Román Rosón et al. 2019, Rompani et al. 2017). Thus, the main image-forming pathway in mice consists of a handful of parallel channels, comparable to the number found in primates (Nassi & Callaway 2009). However, unlike the parvo-, magno- and koniocellular channels in primates, only dLGN core and dLGN shell subchannels have been identified in mice (Kirschensteiner & Guido 2017) (**Figure 4**). While inputs to the dLGN core originate from multiple different types of GCs, most inputs to the dLGN shell come from ON-OFF direction–selective ganglion cells (ON-OFF DSGCs) located in the contralateral retina (Dhande et al. 2015, Okigawa et al. 2021). ON-OFF DSGCs account for a large, 15% stake of GCs specialized for processing image motion in all cardinal directions (Cruz-Martín et al. 2014, Ellis et al. 2016, Kay et al. 2011). Outputs from the dLGN shell are carried forward to V1, where they terminate in P_{M2+} of L1 (Cruz-Martín et al. 2014, Ji et al. 2015) (**Figure 2*d***). It is important to stress, however, that the geniculocortical pathway, even the substream via the dLGN shell, is functionally not a labeled line but combines synaptic inputs from different GC types converging onto single dendrites (Liang et al. 2018).

Colliculo-Thalamo-Cortical Network

Alongside the retino-geniculocortical pathway, visual information reaches cortex through a parallel route via the SC and the LP. Direct retinal inputs to LP are sparse and largely derive from nonimage-forming, melanopsin-expressing GCs (Allen et al. 2016). Transsynaptic retrograde tracing of retinal GCs from the LP in *Ntsr1-GN209Cre* mice, which selects for LP-projecting wide-field neurons in the SC (Gale & Murphey 2014, 2018), labeled small ON, OFF, and transient ON-alpha GCs (Goetz et al. 2022, Reinhard et al. 2019). Notably, cell types distinct from ON-OFF DSGCs innervate the dLGN shell (Okigawa et al. 2021).

Similar to carnivores and primates, the LP is divided into anatomically and functionally discrete parts (Baldwin et al. 2017). In mice, the subdivisions are distinguished as retinotopically distinct maps in the posterior, anterior, and medial lateral posterior nucleus (pLP, aLP, and mLP) with strong, sparse, and no detectable input from the SC, respectively (Bennett et al. 2019) (**Figure 4**). LP's most prominent connections are with higher areas of visual cortex. They are all reciprocal, feeding forward to L1 and L4–6 and returning to LP from L5 and L6 in loops biased to the main source of the thalamocortical projection (Bennett et al. 2019, Juavinett et al. 2020, Roth et al. 2016). The SC-recipient pLP preferentially connects with the laterointermediate (LI) and postrhinal (POR) ventral stream areas (Bennett et al. 2019). Projections from the aLP are biased to the anterolateral (AL), rostrolateral (RL), posteromedial (PM), and anteromedial (AM) dorsal stream areas while the mLP is connected with the anterior cingulate area and orbitofrontal area (Bennett et al. 2019) (**Figures 1*b*** and **4**). Retinal inputs from the colliculo-thalamo-cortical pathway to V1 are not only indirect but conveyed by projections of the aLP to L1 and L5 (Bennett et al. 2019, Roth et al. 2016, Zhou et al. 2018). Inputs to V1 L1 are strikingly clustered, but unlike inputs from the dLGN shell, they are targeted to IP_{M2-} (D'Souza et al. 2019) (**Figures 2*c*,*d*** and **4**). LP inputs to L1 have functional properties aligned with feedback signals from self-motion (Roth et al. 2016). Clustered LP inputs are not unique to aLP and V1. They also exist in the projections from pLP to L1 of the higher ventral visual areas LM, LI, and POR, where they terminate in P_{M2+} (Meier et al. 2021). Thus, clustered projections to P_{M2+} and IP_{M2-} modules of V1 and

higher visual areas are superimposed onto retinotopic maps of colliculo-thalamo-cortical inputs (Garrett et al. 2014, Roth et al. 2016, Wang & Burkhalter 2007).

CORTICAL CONNECTIONS WITH V1 MODULES

Modular Dorsal and Ventral Cortico-Cortical Networks

Reciprocal connectivity is a characteristic feature of intracortical networks. Channelrhodopsin-2-assisted mapping of synaptic connections (sCRACM) in V1↔LM and V1↔PM circuits showed that monosynaptic connections, which loop back to the source, are present in L2/3, 5, and 6 (Young et al. 2021); are module-specific; and are stronger for FB from LM to P_{M2+} than to IP_{M2-} of V1 (D'Souza et al. 2019). This provides physiological support for the selective innervation of P_{M2+} by FB connections from LM to V1 (D'Souza et al. 2019). Graph theoretical analyses of connections between areas have shown that LM, LI, and POR are interconnected in a ventral stream network, while projections between AL, RL, AM, and PM belong to a dorsal network (Wang et al. 2012). How does the M2 modularity fit into this organization? Similar to the association of the ventral stream area LM with P_{M2+}, FB from the dorsal stream area AL to V1 shows a preference for P_{M2+} (Ji et al. 2015). In contrast, FB from the dorsal area PM to V1 is strongly biased to IP_{M2-} (D'Souza et al. 2019). The selectivity for modules reveals that LM belongs to a ventral P_{M2+} network, while the dorsal network is divided into a dorsal-anterior P_{M2+} substream represented by AL and RL and a dorsal-medial IP_{M2-} substream represented by PM (D'Souza et al. 2021, Ji et al. 2015). The two proposed dorsal substreams are consistent with the functional target specificity (Glickfeld et al. 2013) and the scarcity of connections between AL- and PM-projecting neurons in L2/3 of V1 (Kim et al. 2018). The importance of M2 modules in the network organization is mirrored by the role of the ventral and dorsal P_{M2+} streams in sensory perception, which is distinct from the involvement of the dorsal IP_{M2-} subnetwork in sensory integration and decision-making (Jin & Glickfeld 2020). Additional support derives from cluster analyses of responses to spatiotemporal frequency, speed, and orientation across eight areas, demonstrating that mouse visual cortex is parcellated into at least three distinct functional streams (Han et al. 2022). Multiple dorsal processing streams also exist in primate visual cortex (Kravitz et al. 2011), suggesting that the network architecture is evolutionarily conserved.

Functional Architecture of Dorsal and Ventral Intracortical Networks

Connectomic analyses of intracortical connections have shown that the cortical network is subdivided into ventral and dorsal streams (Wang et al. 2011, 2012). Next, we discuss how these streams intersect with the M2 modularity in V1.

Ventral network. Although we have focused on the clustering of M2 expression in L1 of V1, similar nonuniformities exist in higher visual areas and in auditory and retrosplenial cortex (Meier et al. 2021). Evidently, modularity is a general feature of the cortical architecture in mice and includes areas involved in nonvisual and cognitive functions. Clustered M2 expression is most striking in the ventral areas LM, LI, P, POR, and PORa and less notable in the areas AL and RL of the dorsal P_{M2+} substream (**Figure 1*b–d***). M2 is undetectable in areas A, AM, and PM of the dorsal IP_{M2-} substream, leaving open whether modules may be revealed by other markers (**Figure 1*c***).

Studies in rats have shown that lesions of lateral extrastriate cortex impair visual pattern discrimination, while injury of the posterior parietal cortex diminishes visuospatial perception (Aggleton et al. 1997, Gallardo et al. 1979, McDaniel et al. 1982, Sánchez et al. 1997, Tees 1999). Recordings in mice support this organization and the ventral network's involvement in invariant

representations of static images (Han et al. 2022, Piasini et al. 2021). Recent studies further suggest that the shape of M2-postive patches in ventral cortex corresponds to representations of visual space. Surveys in ventral visual cortex have shown that the shape of P_{M2+} is correlated with anisotropies of the retinotopic maps in V1, LM, LI, and POR (Ji et al. 2015, Meier et al. 2021). While module size remains roughly constant across areas, the number of modules per square degree of visual space decreases up the V1→LM→LI→POR hierarchy (D'Souza et al. 2022, Meier et al. 2021). This demonstrates that individual P_{M2+} are integrating increasingly larger portions of the visual field and are presumably linked to visual processing.

Similar to V1, P_{M2+} in LM, LI, and POR receive input from the dLGN, which for projections to POR originates in the dLGN shell (Meier et al. 2021). Unlike V1, P_{M2+} of LM, LI, and POR also receive input from the LP. However, in contrast to V1, inputs derive from the pLP, not the aLP, which projects to IP_{M2-} of V1 (Bennett et al. 2019, D'Souza et al. 2019) (**Figure 4**). Recordings in pLP have shown that these inputs provide sensitivity for the direction and speed of small spots moving over a stationary background (Bennett et al. 2019). Notably, the pLP inputs were shown to provide direction selectivity (DS) to neurons in POR, which are unaffected by blocking intracortical input from V1 (Beltramo & Scanziani 2019). Thus, the connectivity suggests that P_{M2+} in POR are specialized for the processing of small moving and looming objects.

Ventral areas differ from dorsal areas in their strong reciprocal connectivity with the amygdala (Burgess et al. 2016, Meier et al. 2021), the structure responsible for associating visual stimuli with fear and reward. While similar observations have been made in rat (McDonald & Mascagni 1996), it is unexpected that the connectivity is modular. Unlike dLGN and pLP inputs to P_{M2+}, connections from the basolateral amygdala terminate in L1 IP_{M2-} of LM, LI, P, and POR. Inputs from the amygdala overlap with apical dendrites of L5 amygdala-projecting cells in IP_{M2-} and form module-specific loops, which in POR were shown to carry reward-related information (Burgess et al. 2016, Meier et al. 2021). Although ventral and dorsal areas belong to different streams, the networks are highly interconnected (Gămănuţ et al. 2018). For example, dorsal stream inputs to IP_{M2-} of POR may associate information about objects and locations, providing the spatial context in which objects appear (Furtak et al. 2012). As contexts change in the proportion of threat and reward, POR can be modulated by inputs from the amygdala, which receives input from pLP (Bennett et al. 2019, Wei et al. 2015) (**Figure 4**). The same circuit may also influence IP_{M2-} POR cells that project to medial entorhinal cortex, which enhances the salience of landmark information and alerts to unexpected objects.

Dorsal network. To navigate through the environment, an important task is to compute the direction of global motion from local motion signals and to discriminate external from self-generated visual motion. Powerful cues come from the eyes, which provide optic flow signals from the retina. Extraretinal cues derive from the body and include inputs from muscles, joints, and the vestibular system. Combining these inputs involves communications between geniculocortical, colliculo-thalamo-cortical, intracortical, and cortico-thalamo-cortical networks. Here, we focus on the modular architecture in which visual motion signals are represented in different substreams.

The modular architecture of the dorsal stream can be most effectively linked to visual motion processing. Recordings in *Frmd7* mice, in which DS is disrupted by eliminating asymmetric inhibition of ON-OFF DSGCs by starburst amacrine cells in the retina (Yonehara et al. 2016), have shown that DS for posterior motion is abolished in L2/3 of V1 (Hillier et al. 2017). Retina-derived DS is conveyed to V1 via the dLGN shell, which projects to P_{M2+} of L1 (Cruz-Martín et al. 2014, Ji et al. 2015, Roth et al. 2016). From here, DS is transmitted to apical dendrites of L2/3 neurons, inputs are pooled to enlarge the aperture of RFs, and cells become sensitive for the true direction of coherent motion that underlies perception of the direction of optic flow (Marques et al.

2018). Retina-derived DS is acquired preferentially by RL-projecting neurons (Rasmussen et al. 2020), which reside in P_{M2+} modules of V1 (D'Souza et al. 2021) (**Figure 4**). DS of neighboring PM-projecting V1 neurons (Rasmussen et al. 2020) in IP_{M2-} (D'Souza et al. 2021) is independent of ON-OFF DSRGs and emerges from computations within interlaminar circuits of V1 (Lien & Scanziani 2018). Alternatively, DS of PM-projecting cells may be inherited from aLP, whose cells are tuned to global motion in the direction opposite to the animal's heading direction (Bennett et al. 2019). Visual responses to coherent motion of random dot kinematograms are similar in RL and PM and strongly biased to optic flow in the frontal quadrant of the lower visual field (Sit & Goard 2020). While the sensory representations in RL and PM may be similar, they originate from different sources. In RL, DS originates in the retina, whereas in PM, DS comes from aLP and/or V1. The different networks may provide for diverse temporal patterns of DS. But perhaps the real reason for the segregation into distinct modules of V1 is that optic flow signals from P_{M2+} that are sent to RL may be tied to the movements of the eyes, while those from IP_{M2-} addressed to PM are not. Because eye movements rarely occur in the absence of head movements (Meyer et al. 2020), optic flow is encoded in an eye/head-centered reference frame. In contrast, optic flow signals in PM are linked to translations/rotations of the visual scene while bending the trunk during self-motion and are encoded in a body-centered reference frame. In agreement with this proposal, recordings in freely moving rats have shown that neurons that encode head/neck posture are found in lateral posterior parietal cortex, where RL is located. In contrast, cells tuned to the posture of the trunk are clustered more medially in putative PM or AM, where spatiotemporal frequency tuning is matched to the frequencies known to elicit turning of the head and body (Andermann et al. 2011, Mimica et al. 2018). Both of these areas receive input from aLP (**Figure 4**), whose activity in the dark is modulated by eye movements and self-motion (Bennett et al. 2019). RL and PM not only receive input from P_{M2+} and IP_{M2-} in V1, respectively, but also feed back to the source in a like-to-like fashion (D'Souza et al. 2019, 2021). In this way, P_{M2+} V1 neurons combine dLGN shell→P_{M2+} FF and aLP→RL→P_{M2+} dorsal P_{M2+} substream FB inputs (**Figure 4**) to encode conjunctive eye/head and body postures. This conversion may be used to update the registration of eye-centered and body-centered frames during visually guided navigation and extract spatial position and heading information that is not available from dLGN inputs alone (Diamanti et al. 2021). In contrast, IP_{M2-} V1 neurons integrate FF input from aLP→IP_{M2-} and dorsal IP_{M2-} substream FB signals from aLP→PM→IP_{M2-} to predict optic flow based on active motor output during spatial navigation that depends on areas of the posterior parietal cortex (Leinweber et al. 2017, Minderer et al. 2019).

TRANSTHALAMIC NETWORK

Up to this point, the discussion has followed the classic scheme of distributed hierarchical processing (Felleman & Van Essen 1991). Contextual processing of course involves reciprocal communications between lower and higher areas through direct intracortical connections as well as through transthalamic loops via the LP (Sherman 2016).

Recent studies have shed light on how modular and stream-like architectures intersect with transthalamic and intracortical networks that link V1 with higher visual areas. The data are limited to circuits involving AL and PM (Blot et al. 2021). Because AL and RL belong to the dorsal P_{M2+} substream while PM and AM are part of the dorsal IP_{M2-} substream, we assume that similar circuit architectures apply to all members of the dorsal network. Intracortical connections between V1 and AL (and V1 and RL) are reciprocal, originate from cells in P_{M2+}, and return FB projections to P_{M2+} (D'Souza et al. 2019, 2021). Reciprocal interareal connections between V1 and PM (and V1 and AM) involve IP_{M2-} (D'Souza et al. 2019). Tracings of transthalamic connections have shown

that AL and PM are reciprocally connected with distinct types of LP neurons and receive input from largely overlapping sets of visual and nonvisual cortical areas (Blot et al. 2021).

DS in RL was shown to derive from the retina and is conveyed via the dLGN shell and P_{M2+} of V1 to the higher visual area in the posterior parietal cortex (Rasmussen et al. 2020). A similar pathway has been shown to carry optic flow information from V1 to L1 of AL (Blot et al. 2021). This intracortical dorsal P_{M2+} stream of information is purely visual and is unaffected by the animal's running speed (Blot et al. 2021). In parallel with this intracortical stream, a transthalamic pathway originating from IP_{M2-} in V1 may descend subcortically to aLP, which in turn projects back up the hierarchy to AL (**Figure 4**). Unlike intracortical connections, this transthalamic pathway carries optic flow signals, which are modulated by running speed (Blot et al. 2021). This organization suggests that the transthalamic loop may signal "discrepancies between the expected optic flow based on the animal's own movement and the actual visual motion in the environment" and thus "distinguish external visual stimuli from self-generated visual feedback" (Blot et al. 2021, p. 2005). In contrast, transthalamic projections to PM carry a wide range of visuomotor signals, which are more relevant to processing high-spatial-frequency information (Andermann et al. 2011, Han et al. 2022, Marshel et al. 2011).

CORTICAL HIERARCHY

So far we have discussed how the M2 scaffolding in L1 of V1 imposes rules for organizing thalamocortical, corticocortical, and cortico-thalamo-cortical networks. Evidence suggests that the P_{M2+} and IP_{M2-} modules appear to route FF and FB information into three cortical streams/substreams: P_{M2+} ventral, P_{M2+} dorsal posterior parietal, and IP_{M2-} dorsomedial. A model of the connectivity of visual areas in monkeys suggests that processing in ventral and dorsal streams is hierarchical (Markov et al. 2014b). For this reason, the following discussion focuses on whether a similar organization exists in mouse visual cortex and whether the generative networks associated with P_{M2+} and IP_{M2-} exhibit hierarchical and nonhierarchical features (Felleman & Van Essen 1991).

Vision emerges from a constructive process in which feature-selective responses of retinal GCs converge onto image-forming afferent channels, which in the cortex feed into an areal hierarchy that integrates contours, fields of motion, and surfaces in progressively larger RFs. Hierarchical order can be derived from the laminar distribution of cell bodies and axons of interareal connections in primate visual cortex (Felleman & Van Essen 1991). FF pathways were defined as projections originating from PCs in L2/3 and terminating in L4. FB projections originate from deep layers; terminate in L1–2/3, 5, and 6; and avoid L4. Lateral pathways originate in superficial and deep layers and terminate in L1–6. While a structural hierarchy provides a framework for explaining response complexification, binary criteria are insufficient to derive an unambiguous processing hierarchy. The reason for this is the high density of area-to-area connections and the large number of equally valid sequences with the minimal number of violations of FF/FB relationships between reciprocally connected pairs (Hilgetag et al. 1996). To solve this problem, Markov et al. (2014a) used projection weights, expressed as the ratio of retrogradely labeled supragranular cells to all labeled cells in the source area, as an index of hierarchical distance.

Cortical hierarchies have also been identified in rodent visual cortex. Anterograde tracings in rat showed that most interareal pathways labeled axons in L1–6, resembling lateral connections of primates (Coogan & Burkhalter 1993). Nevertheless, connections showed preferences for L4 and L1, signatures for FF and FB projections, respectively. In a quantitative study, Harris et al. (2019) examined the laminar patterns of axonal projections originating in each of 43 cortical areas of mouse neocortex. Using a clustering analysis, they identified nine termination patterns, each representing either a FF or FB connection. A hierarchy was generated by minimizing the number

of violations of the rule that a FF pathway must be reciprocated by a FB pathway and assigning a hierarchy score to each area, which accounts for the number of outgoing FF and incoming FB pathways from a given area. While the scheme implies directed FF and FB information flow, the analysis omitted lateral connections, which may have contributed to a shallow hierarchy.

A recent analysis of the mouse visual cortical network included FF, FB, and lateral connections to derive an index for hierarchical distance (D'Souza et al. 2022). The authors reasoned that if axonal projections from area A to areas C and D provide information about the hierarchical distance between C and D, then projections from another area, B, must return the same distance value between C and D (D'Souza et al. 2022, Vezoli et al. 2021). The ratio of the optical density of axonal terminations in L2–4 to the total axonal density in L1–4 was used for quantification. This approach provides a graded metric, avoids defining connections based on termination patterns of individual pathways, and uses a binary measure to construct the hierarchy. The analysis showed that for reciprocally connected pairs, the more FF a connection is in one direction, the more FB it is in the return pathway. Furthermore, a beta regression model used to obtain hierarchical level values for each of ten visual areas showed that the hierarchical distance, calculated as the difference between the hierarchical levels of any two areas, was predictive of the laminar projection patterns between the two areas. Moreover, interareal pathways could be identified as FF, FB, or lateral based on the hierarchical levels of the corresponding areas. Thus, the cortical network includes multiple hierarchies between select groups of areas. Importantly, it contains various lateral connections that implement a nonhierarchical flow of information. Recordings in mice have shown that RF size grows larger and response onset is more delayed at increasingly higher levels of the hierarchy (D'Souza et al. 2022, Murgas et al. 2020, Siegle et al. 2021), indicating that the anatomical hierarchy is consistent with a physiological hierarchy.

Cellular- and circuit-level properties are constrained by hierarchical rules. sCRACM studies in ex vivo slices of mouse visual cortex showed that the relative synaptic excitation of PV+ interneurons and neighboring PCs by interareal pathways depends on the hierarchical position of areas (D'Souza et al. 2016, Yang et al. 2013). Excitatory interareal input to L2/3 PV+ cells normalized to the activation of a neighboring PC increased with increasing hierarchical distance in the FF direction and decreased in the FB direction. This finding implicates PV+ cells in counterbalancing excitation and differential scaling of the gain in FF and FB pathways in relation to the total excitatory input to PCs at a given stage of the hierarchy (D'Souza & Burkhalter 2017).

In rodents, L1 is not the proverbial cortical FB layer, but it receives assorted inputs from FF, FB, and lateral interareal connections (D'Souza et al. 2022). The reason for its magnetism comes from its role in dendritic integration shaped by local interneurons and muscarinic acetylcholine receptors in apical dendrites of PCs (Larkum 2013, Schuman et al. 2021, Williams & Fletcher 2019). L1 inputs to apical dendrites can generate spikes whose firing patterns can be modified by coincident input to proximal dendrites, a cellular mechanism correlated with alterations in sensory perception and learning (Doron et al. 2020, Manita et al. 2015, Takahashi et al. 2016). As thalamocortical and FB inputs are often clustered, the activity of subpopulations of V1 neurons can be preferentially influenced and information selectively routed through the ventral P_{M2+} and dorsal P_{M2+} and IP_{M2-} substreams (**Figure 4**). The ventral P_{M2+} stream comprising LM, P, LI, and POR traverses ten hierarchical levels, while only eight levels are crossed by the P_{M2+} (AL, RL, A) and IP_{M2-} (PM, AM) dorsal substreams, whose areas are strongly linked by a larger number of lateral connections (D'Souza et al. 2022) (**Figure 5**). This organization suggests that, in the dorsal stream, low-dimensional representations are achieved in fewer steps than in the ventral stream. Interactions between ventral and dorsal streams likely occur through lateral connections from P_{M2+} and may play a role in updating the registration of eye-centered and body-centered frames during visually guided navigation (**Figures 4** and **5**).

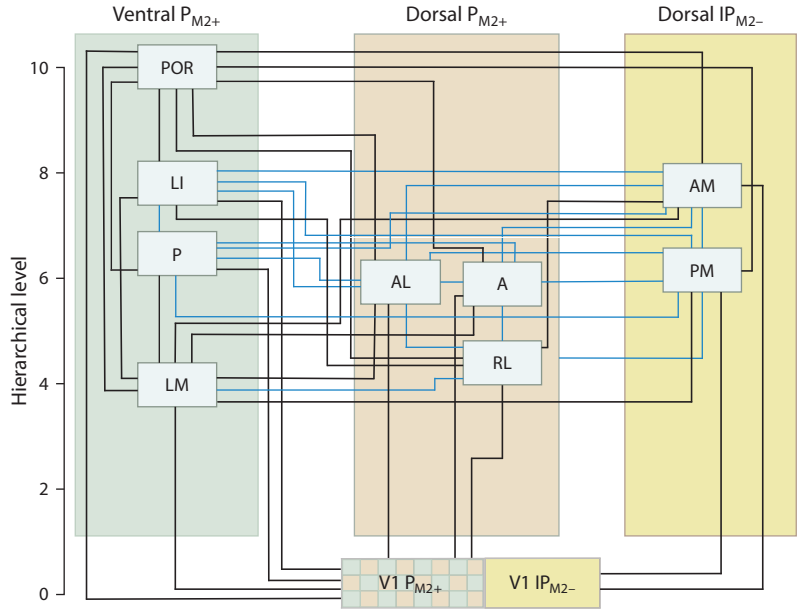

Figure 5

Hierarchical organization of mouse visual cortex, with hierarchical levels estimated using a beta regression model and areas separated into ventral P_{M2+}, dorsal P_{M2+}, and dorsal IP_{M2-} streams based on connection weights and preferences for targeting M2+ and M2− modules. Hierarchical levels were determined such that V1 was set to 0, and the difference between the level values of any two areas best predicted the optical density ratio of termination patterns of interareal projections between the areas. Black lines interconnect areas with significantly different hierarchical levels and are therefore interpreted as FF/FB connections; blue lines interconnect areas that lack a significant difference in their level values and are therefore considered to be lateral connections. Note that the P_{M2+} module in V1 is linked to areas in both dorsal and ventral streams, whereas IP_{M2-} communicates preferentially with the dorsal stream. Abbreviations: A, anterior area; AL, anterolateral; AM, anteromedial; FB, feedback; FF, feedforward; IP_{M2-}, M2-negative interpatch; LI, laterointermediate; LM, lateromedial; M2, M2 muscarinic acetylcholine receptor; P, posterior area; PM, posteromedial; P_{M2+}, M2-positive patch; POR, postrhinal; RL, rostrolateral; V1, primary visual cortex.

The ubiquity of L1 terminations indicates that the mouse cortical network does not comprise a strict sequence of areas in which an unambiguous FF pathway carrying retinal signals is reciprocated by a FB connection providing top-down control; instead, most areal pairs are linked by pathways carrying signals in both directions. This view is consistent with the proposal that a strict areal hierarchy is not required for predictive processing. In other words, predictions and prediction errors can be exchanged in both directions, depending on the sensory modality being engaged (Keller & Mrsic-Flogel 2018). In mouse visual cortex, multiple hierarchies are embedded within the densely interconnected lateral network. For example, the hierarchical networks V1↔LM↔P↔POR, V1↔AL↔POR, and V1↔RL↔AM are connected to each other via numerous lateral connections (D'Souza et al. 2022) (**Figure 5**). Such an organization raises the possibility of a system by which specific functional hierarchies can be dynamically associated through lateral nonhierarchical connections.

DISCLOSURE STATEMENT

The authors are not aware of any affiliations, memberships, funding, or financial holdings that might be perceived as affecting the objectivity of this review.

ACKNOWLEDGMENTS

We thank former members of the Burkhalter lab, in particular Pawan Bista, Enquan Gao, Katia Valkova, and Quanxing Wang. We also would like to thank Henry Kennedy, Ken Knoblauch, Kevan Martin, and David Van Essen for many useful discussions. This work was supported by the National Institutes of Health grants RO1EY016184, RO1EYRO1020523, RO1EY022090, RO1EY027383, and R21EY027946.

LITERATURE CITED

Adams DL, Horton JC. 2009. Ocular dominance columns: enigmas and challenges. *Neuroscientist* 15(1):62–77

Aggleton JP, Keen S, Warburton EC, Bussey TJ. 1997. Extensive cytotoxic lesions involving both the rhinal cortices and area TE impair recognition but spare spatial alternation in the rat. *Brain Res. Bull.* 43(3):279–87

Ahmadlou M, Zweifel LS, Heimel JA. 2018. Functional modulation of primary visual cortex by the superior colliculus in the mouse. *Nat. Commun.* 9:3895

Allen AE, Procyk CA, Howarth M, Walmsley L, Brown TM. 2016. Visual input to the mouse lateral posterior and posterior thalamic nuclei: photoreceptive origins and retinotopic order. *J. Physiol.* 594(7):1911–29

Andermann ML, Ferlin AM, Roumis DK, Glickfeld LL, Reid RC. 2011. Functional specialization of mouse higher visual cortical areas. *Neuron* 72:1025–39

Baden T, Berens P, Franke K, Román Rosón M, Bethge M, Euler T. 2016. The functional diversity of retinal ganglion cells in the mouse. *Nature* 529(7586):345–50

Baldwin MKL, Balaram P, Kaas JH. 2017. The evolution and functions of nuclei of the visual pulvinar in primates. *J. Comp. Neurol.* 525(15):3207–26

Beltramo R, Scanziani M. 2019. A collicular visual cortex: neocortical space for an ancient midbrain visual structure. *Science* 363(6422):64–69

Bennett C, Gale SD, Garrett ME, Newton ML, Callaway EM, et al. 2019. Higher-order thalamic circuits channel parallel streams of visual information in mice. *Neuron* 102(2):477–92

Berry MJ II, Tkacik G. 2020. Clustering of neural activity: a design principle for population codes. *Front. Comput. Neurosci.* 14:20

Bickford ME, Zhou N, Krahe TE, Govindaiah G, Guido W. 2015. Retinal and tectal "driver-like" inputs converge in the shell of the mouse dorsal lateral geniculate nucleus. *J. Neurosci.* 35(29):10523–34

Blot A, Roth MM, Gasler I, Javadzadeh M, Imhof F, Hofer SB. 2021. Visual intracortical and transthalamic pathways carry distinct information to cortical areas. *Neuron* 109(12):1996–2008.e6

Bonin V, Histed MH, Yurgenson S, Reid RC. 2011. Local diversity and fine-scale organization of receptive fields in mouse visual cortex. *J. Neurosci.* 31(50):18506–21

Burgess CR, Ramesh RN, Sugden AU, Levandowski KM, Minnig MA, et al. 2016. Hunger-dependent enhancement of food cue responses in mouse postrhinal cortex and lateral amygdala. *Neuron* 91(5):1154–69

Casagrande VA, Yazar F, Jones KD, Ding Y. 2007. The morphology of the koniocellular axon pathway in the macaque monkey. *Cereb. Cortex* 17(10):2334–45

Chaplin TA, Margrie TW. 2020. Cortical circuits for integration of self-motion and visual-motion signals. *Curr. Opin. Neurobiol.* 60:122–28

Chklovskii DB, Koulakov AA. 2004. Maps in the brain: What can we learn from them? *Annu. Rev. Neurosci.* 27:369–92

Cohen-Kashi Malina K, Tsivourakis E, Kushinsky D, Apelblat D, Shtiglitz S, et al. 2021. NDNF interneurons in layer 1 gain-modulate whole cortical columns according to an animal's behavioral state. *Neuron* 109:2150–64.e5

Coogan TA, Burkhalter A. 1993. Hierarchical organization of areas in rat visual cortex. *J. Neurosci.* 13(9):3749–72

Cruz-Martín A, El-Danaf RN, Osakada F, Sriram B, Dhande OS, et al. 2014. A dedicated circuit links direction-selective retinal ganglion cells to the primary visual cortex. *Nature* 507(7492):358–61

da Costa NM, Martin KAC. 2010. Whose cortical column would that be? *Front. Neuroanat.* 4:16

Dhande OS, Stafford BK, Lim J-HA, Huberman AD. 2015. Contributions of retinal ganglion cells to subcortical visual processing and behaviors. *Annu. Rev. Vis. Sci.* 1:291–328

Diamanti EM, Reddy CB, Schröder S, Muzzu T, Harris KD, et al. 2021. Spatial modulation of visual responses arises in cortex with active navigation. *eLife* 10:e63705

Disney AA, Domakonda KV, Aoki C. 2006. Differential expression of muscarinic acetylcholine receptors across excitatory and inhibitory cells in visual cortical areas V1 and V2 of the macaque monkey *J. Comp. Neurol.* 499:49–63

Doron G, Shin JN, Takahashi N, Drüke M, Bocklisch C, et al. 2020. Perirhinal input to neocortical layer 1 controls learning. *Science* 370(6523):eaaz3136

Dräger UC. 1974. Autoradiography of tritiated proline and fucose transported transneuronally from the eye to the visual cortex in pigmented and albino mice. *Brain Res.* 82(2):284–92

Dräger UC. 1975. Receptive fields of single cells and topography in mouse visual cortex. *J. Comp. Neurol.* 160(3):269–90

D'Souza RD, Bista P, Meier AM, Ji W, Burkhalter A. 2019. Spatial clustering of inhibition in mouse primary visual cortex. *Neuron* 104(3):588–600.e5

D'Souza RD, Burkhalter A. 2017. A laminar organization for selective cortico-cortical communication. *Front. Neuroanat.* 11:71

D'Souza RD, Ji W, Burkhalter A. 2021. *A modular organization of looped interareal and thalamocortical pathways in mouse visual cortex*. Paper presented at the 50th Annual Meeting of the Society for Neuroscience, virtual, Novemb. 8

D'Souza RD, Meier AM, Bista P, Wang Q, Burkhalter A. 2016. Recruitment of inhibition and excitation across mouse visual cortex depends on the hierarchy of interconnecting areas. *eLife* 5:e19332

D'Souza RD, Wang Q, Ji W, Meier AM, Kennedy H, et al. 2022. Hierarchical and nonhierarchical features of the mouse visual cortical network. *Nat. Commun.* 13:503

Egger R, Schmitt AC, Wallace DJ, Kerr JND. 2015. Robustness of sensory-evoked excitation is increased by inhibitory inputs to distal apical tuft dendrites. *PNAS* 112(45):14072–77

Ellis EM, Gauvain G, Sivyer B, Murphy GJ. 2016. Shared and distinct retinal input to the mouse superior colliculus and dorsal lateral geniculate nucleus. *J. Neurophysiol.* 116(2):602–10

Escobar MI, Pimienta H, Caviness VS, Jacobson M, Crandall JE, Kosik KS. 1986. Architecture of apical dendrites in the murine neocortex: dual apical dendritic systems. *Neuroscience* 17(4):975–89

Federer F, Ta'afua S, Merlin S, Hassanpour MS, Angelucci A. 2021. Stream-specific feedback inputs to the primate primary visual cortex. *Nat. Commun.* 12:228

Felleman DJ, Van Essen DC. 1991. Distributed hierarchical processing in the primate cerebral cortex. *Cereb. Cortex* 1(1):1–47

Fitzpatrick D, Itoh K, Diamond IT. 1983. The laminar organization of the lateral geniculate body and the striate cortex in the squirrel monkey (*Saimiri sciureus*). *J. Neurosci.* 3(4):673–702

Furtak SC, Ahmed OJ, Burwell RD. 2012. Single neuron activity and theta modulation in postrhinal cortex during visual object discrimination. *Neuron* 76(5):976–88

Gale SD, Murphey GJ. 2014. Distinct representation and distribution of visual information by specific cell types in mouse superficial superior colliculus. *J. Neurosci.* 34(40):13458–71

Gale SD, Murphey GJ. 2018. Distinct cell types in the superior colliculus project to the dorsal lateral geniculate and the lateral posterior thalamic nuclei. *J. Neurophysiol.* 120:1286–92

Gallardo L, Mottles M, Vera L, Carrasco MA, Torrealba F, et al. 1979. Failure by rats to learn a visual conditional discrimination after lateral peristriate cortical lesions. *Psychobiology* 7(2):173–77

Gămănuţ R, Kennedy H, Toroczkai Z, Ercsey-Ravasz M, Van Essen DC, et al. 2018. The mouse cortical connectome, characterized by an ultra-dense cortical graph, maintains specificity by distinct connectivity profiles. *Neuron* 97(3):698–715

Garrett ME, Nauhaus I, Marshel JH, Callaway EM. 2014. Topography and areal organization of mouse visual cortex. *J. Neurosci.* 34(37):12587–600

Girman SV, Sauvé Y, Lund RD. 1999. Receptive field properties of single neurons in rat primary visual cortex. *J. Neurophysiol.* 82:301–11

Glickfeld LL, Andermann ML, Bonin V, Reid RC. 2013. Cortico-cortical projections in mouse visual cortex are functionally target specific. *Nat. Neurosci.* 16:219–26

Goetz J, Jessen ZF, Jacobi A, Mani A, Cooler S, et al. 2022. Unified classification of mouse retinal ganglion cells using function, morphology, and gene expression. *Cell Rep*. 40(2):111040

Han X, Vermaercke B, Bonin V. 2022. Diversity of spatiotemporal coding reveals specialized visual processing streams in the mouse cortex. *Nat. Commun.* 13:3249

Harris JA, Mihalas S, Hirokawa KE, Whitesell JD, Choi H, et al. 2019. Hierarchical organization of cortical and thalamic connectivity. *Nature* 575(7781):195–202

Hilgetag CC, O'Neill MA, Young MP. 1996. Indeterminate organization of the visual system. *Science* 271(5250):776–77

Hillier D, Fiscella M, Drinnenberg A, Trenholm S, Rompani SB, et al. 2017. Causal evidence for retina-dependent and -independent visual motion computations in mouse cortex. *Nat. Neurosci.* 20(7):960–68

Horton JC, Adams DL. 2005. The cortical column: a structure without a function. *Philos. Trans. R. Soc. B* 360(1456):837–62

Ichinohe N, Fujiyama F, Kaneko T, Rockland KS. 2003. Honeycomb-like mosaic at the border of layers 1 and 2 in the cerebral cortex. *J. Neurosci.* 23(4):1372–82

Innocenti GM, Vercelli A. 2010. Dendritic bundles, minicolumns, columns, and cortical output units. *Front. Neuroanat.* 4:11

Jang J, Song M, Paik S-B. 2020. Retino-cortical mapping ratio predicts columnar and salt-and-pepper organization in mammalian visual cortex. *Cell Rep.* 30(10):3270–79.e3

Ji W, Gămănuţ R, Bista P, D'Souza RD, Wang Q, Burkhalter A. 2015. Modularity in the organization of mouse primary visual cortex. *Neuron* 87(3):632–43

Jiang X, Wang G, Lee AJ, Stronetta RL, Zhu JJ. 2013. The organization of two new interneuronal circuits. *Nat. Neurosci.* 16(2):210–18

Jin J, Wang Y, Swadlow HA, Alonso JM. 2011. Population receptive fields of ON and OFF thalamic inputs to an orientation column in visual cortex. *Nat. Neurosci.* 14(2):232–38

Jin M, Glickfeld LL. 2020. Mouse higher visual areas provide both distributed and specialized contributions to visually guided behaviors. *Curr. Biol.* 30:4682–92.e7

Juavinett AL, Kim EJ, Collins HC, Callaway EM. 2020. A systematic topographical relationship between mouse lateral posterior thalamic neurons and their visual cortical projection targets. *J. Comp. Neurol.* 528(1):99–111

Karimi A, Odenthal J, Drawitsch F, Boergens KM, Helmstaedter M. 2020. Cell-type specific innervation of cortical pyramidal cells at their apical dendrites. *eLife* 9:e46876

Kay JN, De la Huerta I, Kim I-J, Zhang Y, Yamagata M, et al. 2011. Retinal ganglion cells with distinct directional preferences differ in molecular identity, structure, and central projections. *J. Neurosci.* 31(21):7753–62

Keller GB, Mrsic-Flogel TD. 2018. Predictive processing: a canonical cortical computation. *Neuron* 100(2):424–35

Kerschensteiner D. 2022. Feature detection by retinal ganglion cells. *Annu. Rev. Vis. Sci*. 8:135–69

Khan AG, Hofer SB. 2018. Contextual signals in visual cortex. *Curr. Opin. Neurobiol.* 52:131–38

Kim M-H, Znamenskiy P, Iacaruso MF, Mrsic-Flogel TD. 2018. Segregated subnetworks of intracortical projection neurons in primary visual cortex. *Neuron* 100(6):1313–21.e6

Kirschensteiner D, Guido W. 2017. Organization of the dorsal lateral geniculate nucleus in the mouse. *Vis. Neurosci.* 34:e008

Kondo S, Yoshida T, Ohki K. 2016. Mixed functional microarchitectures for orientation selectivity in the mouse primary visual cortex. *Nat. Commun.* 7(1):13210

Kravitz DJ, Saleem KS, Baker CI, Mishkin M. 2011. A new neural framework for visuospatial processing. *Nat. Rev. Neurosci.* 12(4):217–30

Kremkow J, Jin J, Wang Y, Alonso JM. 2016. Principles underlying sensory map topography in primary visual cortex. *Nature* 533(7601):52–57

Laing RJ, Turecek J, Takahata T, Olavarria JF. 2015. Identification of eye-specific domains and their relation to callosal connections in primary visual cortex of Long Evans rats. *Cereb. Cortex* 25(10):3314–29

Larkum M. 2013. A cellular mechanism for cortical associations: an organizing principle for the cerebral cortex. *Trends Neurosci.* 36:141–51

Lee K-S, Huang X, Fitzpatrick D. 2016. Topology of ON and OFF inputs in visual cortex enables an invariant columnar architecture. *Nature* 533(7601):90–94
Leinweber M, Ward DR, Sobczak JM, Attinger A, Keller GB. 2017. A sensorimotor circuit in mouse cortex for visual flow predictions. *Neuron* 95(6):1420–32.e5
Liang L, Fratzl A, Goldey G, Ramesh RN, Sugden AU, et al. 2018. A fine-scale functional logic to convergence from the retina to thalamus. *Cell* 173:1343–55
Lien AD, Scanziani M. 2013. Tuned thalamic excitation is amplified by visual cortical circuits. *Nat. Neurosci.* 16(9):1315–23
Lien AD, Scanziani M. 2018. Cortical direction selectivity emerges at convergence of thalamic synapses. *Nature* 558(7708):80–86
Loomba S, Straehle J, Gangadharan V, Heike N, Khalifa A, et al. 2022. Connectomic comparison of mouse and human cortex. *Science* 377(6602):eabo0924
Mangini NJ, Pearlman AL. 1980. Laminar distribution of receptive field properties in the primary visual cortex of the mouse. *J. Comp. Neurol.* 193(1):203–22
Manita S, Suzuki T, Homma C, Matsumoto T, Odagawa M, et al. 2015. A top-down cortical circuit for accurate sensory perception. *Neuron* 86(5):1304–16
Markov NT, Ercsey-Ravasz MM, Ribeiro Gomes AR, Lamy C, Magrou L, et al. 2014a. A weighted and directed interareal connectivity matrix for macaque cerebral cortex. *Cereb. Cortex* 24(1):17–36
Markov NT, Vezoli J, Chameau P, Falchier A, Quilodran R, et al. 2014b. Anatomy of hierarchy: feedforward and feedback pathways in macaque visual cortex. *J. Comp. Neurol.* 522:225–59
Marques T, Nguyen J, Fioreze G, Petreanu L. 2018. The functional organization of cortical feedback inputs to primary visual cortex. *Nat. Neurosci.* 21(5):757–64
Marshel JH, Garrett ME, Nauhaus I, Callaway EM. 2011. Functional specialization of seven mouse visual cortical areas. *Neuron* 72:1040–54
Martersteck E, Hirokawa KE, Evarts M, Bernard A, Duan X, et al. 2017. Diverse central projection patterns of retinal ganglion cells. *Cell Rep.* 18(8):2058–72
Maruoka H, Nakagawa N, Tsuruno S, Sakai S, Yoneda T, Hosoya T. 2017. Lattice system of functionally distinct cell types in the neocortex. *Science* 358(6363):610–15
McDaniel WF, Coleman J, Lindsay JF. 1982. A comparison of lateral peristriate and striate neocortical ablations in the rat. *Behav. Brain Res.* 6(3):249–72
McDonald AJ, Mascagni F. 1996. Cortico-cortical and cortico-amygdaloid projections of the rat occipital cortex: a *Phaseolus vulgaris* leucoagglutinin study. *Neuroscience* 71(1):37–54
Meier AM, Wang Q, Ji W, Ganachaud J, Burkhalter A. 2021. Modular network between postrhinal visual cortex, amygdala, and entorhinal cortex. *J. Neurosci.* 41(22):4809–25
Meyer AF, O'Keefe J, Poort J. 2020. Two distinct types of eye-head coupling in freely moving mice. *Curr. Biol.* 30(11):2116–30.e6
Mimica B, Dunn BA, Tombaz T, Bojja VPTNCS, Whitlock JR. 2018. Efficient cortical coding of 3D posture in freely behaving rats. *Science* 362(6414):584–89
Minderer M, Brown KD, Harvey CD. 2019. The spatial structure of neural encoding in mouse posterior cortex during navigation. *Neuron* 102(1):232–48.e11
Molnár Z, Rockland KS. 2020. Cortical columns. In *Neural Circuit and Cognitive Development*, ed. J Rubenstein, P Rakic, B Chen, KY Kwan, pp. 103–26. San Diego, CA: Academic. 2nd ed.
Morin LP, Studholme KM. 2014. Retinofugal projections in the mouse. *J. Comp. Neurol.* 522(16):3733–53
Mrzljak L, Levey AI, Rakic P. 1996. Selective expression of m2 muscarinic receptor in the parvocellular channel of primate visual cortex. *PNAS* 93:7337–40
Murakami T, Matsui T, Uemura M, Ohki K. 2022. Modular strategy of development of the hierarchical visual network in mice. *Nature* 608:578–85
Murgas KA, Wilson AM, Michael V, Glickfeld LL. 2020. Unique spatial integration in mouse primary visual cortex and higher visual areas. *J. Neurosci.* 40(9):1862–73
Nassi JJ, Callaway EM. 2009. Parallel processing strategies of the primate visual system. *Nat. Rev. Neurosci.* 10(5):360–72
Nauhaus I, Nielsen KJ. 2014. Building maps from maps in primary visual cortex. *Curr. Opin. Neurobiol.* 24:1–6

Ohki K, Chung S, Ch'ng YH, Kara P, Reid RC. 2005. Functional imaging with cellular resolution reveals precise micro-architecture in visual cortex. *Nature* 433(7026):597–603

Ohki K, Chung S, Kara P, Hübener M, Bonhoeffer T, Reid RC. 2006. Highly ordered arrangement of single neurons in orientation pinwheels. *Nature* 442(7105):925–28

Ohki K, Reid RC. 2007. Specificity and randomness in the visual cortex. *Curr. Opin. Neurobiol.* 17(4):401–7

Okigawa S, Yamaguchi M, Ito KN, Takeuchi RF, Morimoto N, Osakada F. 2021. Cell type- and layer-specific convergence in core and shell neurons of the dorsal lateral geniculate nucleus. *J. Comp. Neurol.* 529(8):2099–124

Paik S-B, Ringach DL. 2011. Retinal origin of orientation maps in visual cortex. *Nat. Neurosci.* 14(7):919–25

Pardi MB, Vogenstahl J, Dalmay T, Spanò T, Pu D-L, et al. 2020. A thalamocortical top-down circuit for associative memory. *Science* 370:844–48

Park J, Papoutsi A, Ash RT, Marin MA, Poirazi P, Smirnakis SM. 2019. Contribution of apical and basal dendrites to orientation encoding in mouse V1 L2/3 pyramidal neurons. *Nat. Commun.* 10:5372

Pattadkal JJ, Mato G, van Vreswijk, Priebe NJ, Hansel D. 2018. Emergent orientation selectivity from random networks in mouse visual cortex. *Cell Rep.* 24:2042–50

Peters A, Kara DA. 1987. The neuronal composition of area 17 of rat visual cortex. IV. The organization of pyramidal cells. *J. Comp. Neurol.* 260(4):573–90

Piasini E, Soltuzu L, Muratore P, Caramellino R, Vinken K, et al. 2021. Temporal stability of stimulus representation increases along rodent visual cortical hierarchies. *Nat. Commun.* 12:4448

Ramesh RN, Burgess CR, Sugden AU, Gyetvan M, Andermann ML. 2018. Intermingled ensembles encode stimulus identity or predicted outcome in visual association cortex. *Neuron* 100(4):900–15

Rasmussen R, Matsumoto A, Dahlstrup Sietam M, Yonehara K. 2020. A segregated cortical stream for retinal direction selectivity. *Nat. Commun.* 11:831

Reinhard K, Li C, Do Q, Burke EG, Heynderickx S, Farrow K. 2019. A projection specific logic to sampling visual inputs in mouse superior colliculus. *eLife* 8:e50697

Ringach DL, Mineault PJ, Tring E, Olivas ND, Garcia-Junco-Clemente P, Trachtenberg JT. 2016. Spatial clustering of tuning in mouse primary visual cortex. *Nat. Commun.* 7:12270

Roelfsema PR. 2006. Cortical algorithms for perceptual grouping. *Annu. Rev. Neurosci.* 29:203–27

Roelfsema PR, de Lange FP. 2016. Early visual cortex as a multiscale cognitive blackboard. *Annu. Rev. Vis. Sci.* 2:131–51

Román Rosón M, Bauer Y, Kotkat AH, Berens P, Euler T, Busse L. 2019. Mouse dLGN receives functional input from a diverse population of retinal ganglion cells with limited convergence. *Neuron* 102(2):462–76.e8

Rompani SB, Müller FE, Wanner A, Zhang C, Roth CN, et al. 2017. Different modes of visual integration in the lateral geniculate nucleus revealed by single-cell-initiated transsynaptic tracing. *Neuron* 93:767–76.e6

Roth MM, Dahmen JC, Muir DR, Imhof F, Martini FJ, Hofer SB. 2016. Thalamic nuclei convey diverse contextual information to layer 1 of visual cortex. *Nat. Neurosci.* 19(2):299–307

Saleem AB. 2020. Two stream hypothesis of visual processing for navigation in mouse. *Curr. Opin. Neurobiol.* 64:70–78

Saleem AB, Ayaz A, Jeffery KJ, Harris KD, Carandini M. 2013. Integration of visual motion and location in mouse visual cortex. *Nat. Neurosci.* 16:1864–69

Sánchez RF, Montero VM, Espinoza SG, Díaz E, Canitrot M, Pinto-Hamuy T. 1997. Visuospatial discrimination deficit in rats after ibotenate lesions in anteromedial visual cortex. *Physiol. Behav.* 62(5):989–94

Scala F, Kobak D, Shan S, Bernaerts Y, Laturnus S, et al. 2019. Layer 4 of mouse neocortex differs in cell types and circuit organization between sensory areas. *Nat. Commun.* 10(1):4174

Schneider GE. 1969. Two visual systems. *Science* 163(3870):895–902

Scholl B, Tan AYY, Corey J, Priebe NJ. 2013. Emergence of orientation selectivity in the mammalian visual pathway. *J. Neurosci.* 33(26):10616–24

Schuman B, Dellal S, Prönneke A, Machold R, Rudy B. 2021. Neocortical layer 1: an elegant solution to top-down and bottom-up integration. *Annu. Rev. Neurosci.* 44:221–52

Sherman SM. 2016. Thalamus plays a central role in ongoing cortical functioning. *Nat. Neurosci.* 19(4):533–41

Sherman SM, Guillery RW. 2011. Distinct functions for direct transthalamic corticocortical connections. *J. Neurophysiol.* 106:1068–77

Siegle JH, Jia X, Durand S, Gale S, Bennett C, et al. 2021. Survey of spiking in the mouse visual system reveals functional hierarchy. *Nature* 592(7852):86–92

Sit KK, Goard MJ. 2020. Distributed and retinotopically asymmetric processing of coherent motion in mouse visual cortex. *Nat. Commun.* 11:3565

Siu C, Balsor J, Merlin S, Federer F, Angelucci A. 2021. A direct interareal feedback-to-feedforward circuit in primate visual cortex. *Nat. Commun.* 12:4911

Smith SL, Häusser M. 2010. Parallel processing of visual space by neighboring neurons in mouse visual cortex. *Nat. Neurosci.* 13(9):1144–49

Takahashi N, Oertner TG, Hegeman P, Larkum ME. 2016. Active cortical dendrites modulate perception. *Science* 354:1587–90

Tees RC. 1999. The effects of posterior parietal and posterior temporal cortical lesions on multimodal spatial and nonspatial competencies in rats. *Behav. Brain Res.* 106(1–2):55–73

Tohmi M, Meguro R, Tsukano H, Hishida R, Shibuki K. 2014. The extrageniculate visual pathway generates distinct response properties in the higher visual areas of mice. *Curr. Biol.* 24(6):587–97

Tring E, Duan KK, Ringach DL. 2022. ON/OFF domains shape receptive field structure in mouse visual cortex. *Nat. Commun.* 13:2466

Van Hooser SD, Heimel JA, Chung S, Nelson SB, Toth LJ. 2005. Orientation selectivity without orientation maps in visual cortex of a highly visual mammal. *J. Neurosci.* 25(2):19–28

Vanni S, Hokkanen H, Werner F, Angelucci A. 2020. Anatomy and physiology of macaque visual cortical areas V12, V2, and V5/MT: bases for biologically realistic models. *Cereb. Cortex* 30:3483–517

Vezoli J, Magrou L, Goebel R, Wang X-J, Knoblauch K, et al. 2021. Cortical hierarchy, dual counterstream architecture and the importance of top-down generative networks. *Neuroimage* 225:117479

Wang Q, Burkhalter A. 2007. Area map of mouse visual cortex. *J. Comp. Neurol.* 502(3):339–57

Wang Q, Gao E, Burkhalter A. 2011. Gateways of ventral and dorsal streams in mouse visual cortex. *J. Neurosci.* 31(5):1905–18

Wang Q, Sporns O, Burkhalter A. 2012. Network analysis of corticocortical connections reveals ventral and dorsal processing streams in mouse visual cortex. *J. Neurosci.* 32(13):4386–99

Wei P, Liu N, Zhang Z, Liu X, Tang Y, et al. 2015. Processing of visually evoked innate fear by a non-canonical thalamic pathway. *Nat. Commun.* 6:6756

Williams B, Del Rosario J, Muzzu T, Peelman K, Coletta S, et al. 2021. Spatial modulation of dark versus bright stimulus responses in the mouse visual system. *Curr. Biol.* 31(18):4172–79.e6

Williams SR, Fletcher LN. 2019. A dendritic substrate for the cholinergic control of neocortical output neurons. *Neuron* 101:486–99

Yang W, Carrasquillo Y, Hooks BM, Nerbonne JM, Burkhalter A. 2013. Distinct balance of excitation and inhibition in an interareal feedforward and feedback circuit of mouse visual cortex. *J. Neurosci.* 33(44):17373–84

Yonehara K, Fiscella M, Drinnenberg A, Esposti F, Trenholm S, et al. 2016. Congenital nystagmus gene FRMD7 is necessary for establishing a neuronal circuit asymmetry for direction selectivity. *Neuron* 89(1):177–93

Young H, Belbut B, Baeta M, Petreanu L. 2021. Laminar-specific cortico-cortical loops in mouse visual cortex. *eLife* 10:e59551

Zhou N, Masterson SP, Damron JK, Guido W, Bickford ME. 2018. The mouse pulvinar nucleus links the lateral extrastriate cortex, striatum, and amygdala. *J. Neurosci.* 38(2):347–62